

Original Article

Compartmental Analysis to Predict the Biodistribution of [^{166}Ho]-DOTA-Bevacizumab for Targeted Radiotherapy Purpose

Alireza Khorrami Moghaddam^{1,*}, Amir Hakimi², Alireza Mardanshahi¹, Amir R. Jalilian³, Hossein Amirfakhrian¹, and Hossein Mousavi Anijdan⁴

1- Radiology Department, Allied Faculty, Mazandaran University of Medical Sciences (MazUMS), Sari, Mazandaran, Iran.

2- Health Physics and Dosimetry Research Laboratory, Department of Energy Engineering and Physics, Amirkabir University of Technology, Tehran, Iran.

3- Radiopharmaceutical Research and Development Lab (RRDL), Tehran, Iran.

4- Radiology Department, Allied Faculty, Babol University of Medical Sciences (BUMS), Babol, Mazandaran, Iran.

Received: 28 April 2015

Accepted: 10 August 2015

Keywords:

Compartment analysis,

^{166}Ho -Avastin,

Biodistribution modeling,

Radio targeted therapy,

Internal dosimetry.

ABSTRACT

Purpose- The main aim of this study was to develop the pharmacokinetic model for the colorectal cancer's complex ^{166}Ho -DOTA-Bevacizumab in normal and tumoral rats to analyze of behavior as a new composition for diagnosing and treatment. The use of compartmental analysis allows a mathematical separation of tissues and organs to determine the concentration of activity in each fraction of interest. Biodistribution studies are expensive and difficult to carry out in humans, but such data can be obtained easily in rodents and rat.

Methods- We have developed a physiologically based pharmacokinetic model for scaling up activity concentration in each organ versus time. The mathematical model uses physiological parameters including organ volumes, blood flow rates, and vascular permeability. The compartments (organs) are connected anatomically. This allows the use of scale-up techniques to predict the new complex distribution in humans in each organ.

Results- The concentration of the new complex was measured in various organs at the different times. The behavior of the complex (^{166}Ho -DOTA-Bevacizumab) was modeled as a function of time in various organs. These data was diagrammed as a time function in the separated graph for each organ between 2-96 hours after injection.

Conclusion- The variation of integrated uptake in organs is described with summation of 6-9 exponential terms and it approximated experimental data with 1-2 % precision. As shown in the diagram the mathematical model and biodistribution data in an experiment has a good joint and coincidence and it is a good sign to save time and cost in the next other researches.

1. Introduction

Bevacizumab is a food and drug administration approved, humanized monoclonal antibody that inhibits vascular endothelial growth factor A (VEGF-A), playing an important role in the control of angiogenesis in cancers, including

metastatic colorectal cancer, unrespectable non-squamous non-small cell lung cancer, metastatic breast cancer, glioblastoma, and metastatic renal cell carcinoma [1]. Because of the importance of VEGF-A in the pathology of cancers and the possibility of radionuclide targeting using this antibody, many therapeutic and diagnostic

*** Corresponding Author:**

Alireza Khorrami Moghaddam, PhD

Radiology Department, Allied Faculty, Km17 Sea road, Sari, Mazandaran, Iran.

Tel: (+98) 1133542469

E-mail: ar.khorrami@gmail.com

monoclonal antibodies have been developed as summarized in Table 1. Targeted radiotherapy has been developed over past two decades [2, 3]. In this method, a major proportion of radiation is delivered directly to the cancerous tumor by biological means. The chemical compound with high deposition in tumor is labeled with a beta emitter radioisotope. The high LET (Linear Energy Transfer) of beta particle leads to the destruction of cancer cells while the radioisotope is concentrated inside the tumor. The short range of beta particle spares the healthy tissue surrounding the tumor and the major proportion of the radiation dose is absorbed by the tumor. Among beta emitting radioisotopes is ^{166}Ho with a physical half-life of 26.8 h. Emitted beta ray energies and their abundances are 1853.9 keV (50.3%), 1773.3 keV (48.7%) respectively. Average beta ray energy of 1800 keV renders the penetration depth of 13

mm in soft tissue, making it a good candidate for application in targeted radiotherapy. Besides beta ray, ^{166}Ho emits gamma radiation and conversion electrons with 81 keV energy. Gamma ray at this energy range makes nuclear imaging feasible, while the process of radiotherapy is carried out. Finally, ^{166}Ho decays to stable nuclide ^{166}Er . Holmium, being a Lanthanide metal, concentrates in bone and kidney. This gives the benefit of its absorption in metastatic tissues in bone cancer. As a rule of thumb, concentration of Samarium in metastatic bone tissues is five times higher than in normal tissue [4]. ^{166}Ho -DOTA-Avastin has already been produced in our laboratory [5]. In this work, ^{166}Ho -DOTA-Avastin was developed for possible therapeutic applications (Figure 1) and the variation of its concentration with time in important organs is shown [4, 6, 7].

Table 1. Biological studies performed on some radiolabeled anti-VEGF-A immunomolecules.

Immunomolecule	Radionuclide	Chelator	<i>In vitro</i>	Rodents	Human	Ref.
Bevacizumab	^{86}Y	CHX-A''-DTPA ^a	+	+	—	2
Ranibizumab	^{89}Zr	desferrioxamine	+	+	—	3
Bevacizumab	^{111}In	CHX-A''-DTPA	+	—	—	4
Bevacizumab	^{64}Cu	DOTA ²	+	+	—	5
Bevacizumab	^{111}In	DTPA ^c	+	+	+	6,7
scVEGF ^d	^{68}Ga	NOTA ^e	+	—	—	8
Bevacizumab	$^{206,205}\text{Bi}$	DTPA	+	+	—	9
scVEGF	^{99m}Tc	DTPA	+	+	—	10

^aCHX-A''-DTPA: Isothiocyanate-benzyl-diethylenetetraaminepentaacetic acid.
^bDOTA: 1,4,7,10-tetraazacyclododecane-1,4,7,10-tetraacetic acid.
^cDTPA: diethylenetetraaminepentaacetic acid
^dscVEGF: Engineered single-chain VEGF
^eNOTA: 1,4,7-triazacyclononane-1,4,7-triacetic acid

2. Materials and Methods

2.1. Experimental

Holmium, being a Lanthanide metal, concentrates in bone, especially tissues with high osteoplastic activity; this gives the benefit of its absorption in metastatic tissues in bone cancer. ^{166}Ho was produced by neutron irradiation of 100 μg of natural $^{165}\text{Ho}_2(\text{NO}_3)_3$ (^{165}Ho , 99.99% from ISOTEC Inc.) According to report procedures [8, 9] in the Tehran Research Reactor at a thermal neutron flux of $4 \times 10^{13} \text{ n cm}^{-2} \text{ s}^{-1}$ for 5 days. Sephadex G-50, sodium acetate, phosphate buffer components and methanol were purchased from Sigma-Aldrich Chemical Co. U.K [4].

The specific activity of the produced ^{166}Ho was 3–3.5 GBq/mg after 20 h of irradiation. The irradiated target was dissolved in 200 μl of 1.0 M HCl, to prepare $^{166}\text{HoCl}_3$ and diluted to the appropriate volume with ultra pure water, to produce a stock solution [4]. The mixture was filtered through a 0.22 μm biological filter and sent for use in the radiolabeling step. The radionuclidic purity of the solution was tested for the presence of other radionuclides using beta spectroscopy as well as HPGe spectroscopy for the detection of various interfering beta and gamma emitting radionuclides the radiochemical purity of the $^{166}\text{HoCl}_3$ was checked using two solvent systems for ITLC (A: 10 mM DTPA pH 4 and B: ammonium acetate 10%: methanol (1:1)) [4].

2.2. Biodistribution of ^{166}Ho -Dota-Bevacizumab in Tumor Bearing Mice

The first stage in examining a new pharmaceutical is to study its behavior and effects in the body of a mouse and/or rat. Due to the physiological resemblance between rat and human, the distribution of drugs in a rat body is a good indicator of phenomena appearing in a human body. Thus, the information collected by animal experiments would be applicable for the development of pharmaceuticals for human [9].

In this study, the biological distribution of newly developed ^{166}Ho complex in healthy and tumor bearing rats was evaluated [5].

Colorectal cells were implanted in rat by Xenograft method. Distributions of ^{166}Ho among tissues were determined in untreated mice and in mice with colorectal cancer cells. Briefly, a volume (0.1 ml) of final ^{166}Ho solution containing ($3.5\text{--}3.8 \times 10^6$ Bq) radioactivity was injected intravenously into the dorsal tail vein. The animals were sacrificed at the exact time (2, 4, 24, 48, 96 h) after injection and specific activities of different organs were measured as percentage of injected dose per gram (%ID/g) of tissue using an HPGe detector (%ID/g). The animals were sacrificed by asphyxiation at selected times after injection, the tissues were weighed and their specific activities were determined with scintillation detectors as percentage of injected dose per gram of tissues [4, 5, 10].

The total amount of radioactivity injected into each mouse was measured by counting 1 ml syringe before and after injection in a radiometer with a fixed geometry. ^{166}Ho -DOTA was prepared in two steps. At first, $^{166}\text{HoCl}_3$ was produced by neutron irradiation of an enriched ^{166}Ho sample in a research nuclear reactor. Biodistribution studies of the complex in wild type rats and tumor bearing mice were also determined [11]. The radiolabeled complex was prepared in high radiochemical purity (>99% precipitation method) and specific activity of 278 GBq/mMol and demonstrated significant stability in 4, 25 and 37°C (in the presence of human serum) [4]. Initial biodistribution data showed significant liver accumulation in wild type rat and tumor accumulation in tumor bearing mice of the tracer in 48 h [12]. The properties of

^{166}Ho -DOTA products suggest an efficiently new liver accumulating therapeutic agent in order to overcome possible liver malignancies with the lowest toxicity [5].

To determine biodistribution ^{166}Ho -DOTA-Bevacizumab and $^{166}\text{HoCl}_3$ were administered to normal rats separately [10]. A volume (50 - 100 μl) of final radioactive solution containing 30 ± 5 μCi radioactivity was injected intravenously to rats through their tail vein [5, 10]. The total amount of radioactivity injected into each rat was measured by counting the 1 ml syringe before and after injection in a dose calibrator with a fixed geometry [13]. The animals were killed by CO_2 asphyxiation (after anesthesia induction using propofol/xylazine mixture) at selected times after injection at the exact time intervals (6, 12 and 18 h for both samples) and the specific activities of different organs were calculated [4, 5, 13]. Dissection began by drawing blood from the aorta, followed by collecting heart, spleen, kidneys, liver, intestine, stomach, lung, bone muscle and skin samples [14]. The samples were weighed and their specific activities were determined with an HPGe detector counting the area under the curve of the 80 keV peak [13]. The tissue uptakes were calculated as the percent of the area under the curve of the related photo peak per gram of tissue (ID/g%) [15].

3. Results

The activity concentration in each organ was measured with the use of detectors at specified time (2, 4, 8, 16, 24, 36, 48, 72 and 96 hours) after injection. The results show variation with time, which is depicted in Figure 1. (a to k). The compartmental model [7, 10, 16] was used to produce a mathematical description of these variations. The following equations were obtained for each organ. In each case, $t = 0$ corresponds to the time of injection.

$f_1 = 4.5e^{-0.38t} - (1.8E-3)e^{-5.14t} - (2.8E-3)e^{-0.24t} + (1.44E-1)e^{-0.57t} + 0.45e^{-0.0099t} + (1.96E-4)e^{-0.01t} + 0.16e^{-0.077t}$	1. Blood
$f_2 = -2.094e^{-6.65t} - 0.185e^{-0.04t} - 0.884e^{-0.14t} + (3.44E-3)e^{-0.06t} + 0.95e^{-0.0069t} + (1.96E-3)e^{-0.001t} + 1.7e^{-0.087t}$	2. Bone
$f_3 = 0.14e^{-0.18t} - (5.85E-2)e^{-0.913t} + 0.1e^{-1.15t} + 3.944e^{-1.561t} + 0.185e^{-0.099t} + 1.5e^{-0.001t} + 2.8e^{-0.0461t} - 5.7853865e^{-0.9498t}$	3. Brain
$f_4 = 2.65e^{-0.45t} - (1.85E-4)e^{-5.04t} - (8.84E-7)e^{-0.14t} + (3.44E-3)e^{-0.06t} + 0.95e^{-0.00099t} + (1.96E-3)e^{-0.001t} + 1.7e^{-0.087t}$	4. Heart
$f_5 = 2.28e^{-1.065t} + (1.85E-1)e^{-0.014t} + (9.84E-2)e^{-9.99t} + 0.344e^{-0.789t} + (2E-2)e^{-0.00199t} + (1.96E-3)e^{-0.109t} + 0.76e^{-0.002t}$	5. Intestine
$f_6 = 7.17e^{-0.19t} - 2.185e^{0.973t} + 0.344e^{-0.06t} + 1e^{-0.00099t} + (9.6E-2)e^{-0.001t} + 3.8e^{-0.087t} - 3.9e^{-1.71t} + 0.1e^{-0.001t} - 0.8e^{0.00001t}$	6. Kidney
$f_7 = -(1.7E-3)e^{-0.15t} + 0.179e^{0.04t} - 1.884e^{-0.04t} + (4.4E-2)e^{-9.16t} - 0.5e^{0.0069t} - 0.6e^{-0.004t} + 2.4e^{-0.087t} - 0.22e^{0.037t}$	7. Liver
$f_8 = 0.543e^{-0.38t} - (1.85E-3)e^{-3.14t} - (2.84E-3)e^{-0.04t} + 0.144e^{-0.67t} + 0.45e^{-0.0099t} + (1.96E-4)e^{-0.01t} + 0.25e^{-0.0007t}$	8. Lung
$f_9 = -0.2e^{-0.15t} + 0.179e^{0.0401t} - 1.884e^{-0.04t} + 0.044e^{-4.71t} - 0.5e^{-0.0068t} - 0.6e^{-0.004t} + 2.4e^{-0.088t} + 0.22e^{0.038t}$	9. Spleen
$f_{10} = -0.196e^{-0.18t} - 0.0585e^{-0.913t} + 0.1e^{-1.15t} + 1.944e^{-1.561t} + 0.185e^{-0.00099t} + 1.5e^{0.002t} + 2.8e^{-0.0961t} - 3.78e^{-0.9498t}$	10. Stomach
$f_{11} = 0.304e^{-0.38t} - (1.85E-3)e^{-5.14t} + (2.84E-3)e^{-0.23t} + (1.4E-1)e^{-0.57t} + 0.55e^{-0.0099t} + (2.16E-4)e^{-0.01t} + 0.18e^{-0.077t}$	11. Xyphoid

¹⁶⁶Ho-DOTA imaging performed in the tumor-bearing mice showed a distinct accumulation of the radiotracer in the tumor, while in the first and second hour a background in the liver was absorbed (Figure 1. a to k). Among many Holmium compounds ¹⁶⁶Ho-DOTA-Avastin is proven to be a better choice in the treatment of colorectal cancer [5, 6, 11, and 12].

The criteria to choose this compound was its blood clearance, little concentration in other organs, and practical pain relief in cancer patients.

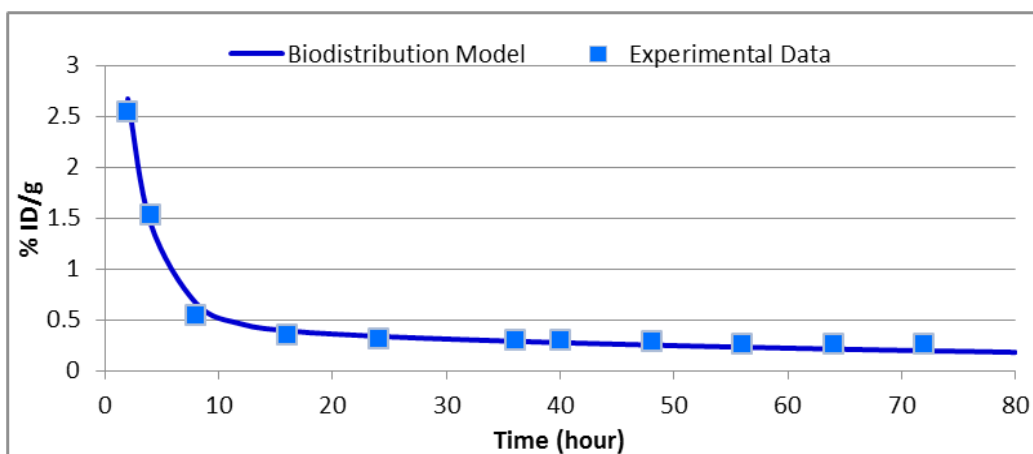


Figure 1. a. Comparison modeling data and biodistribution data for Blood.

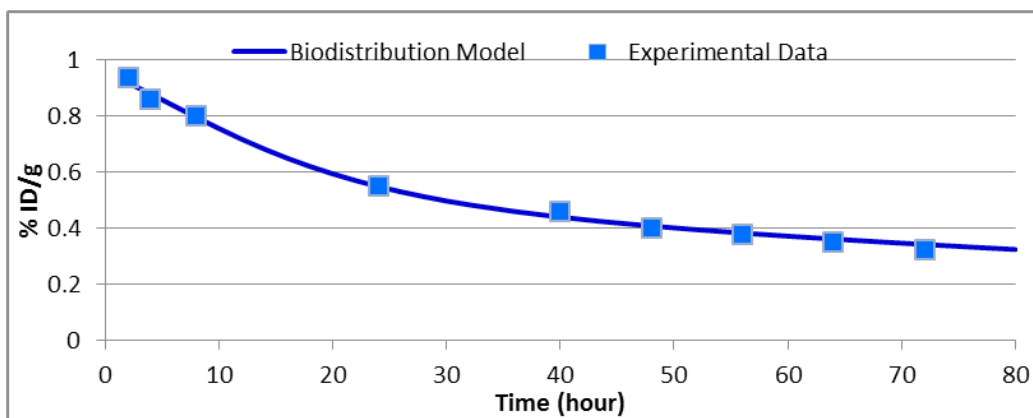


Figure 1. b. Comparison modeling data and biodistribution data for Bone.

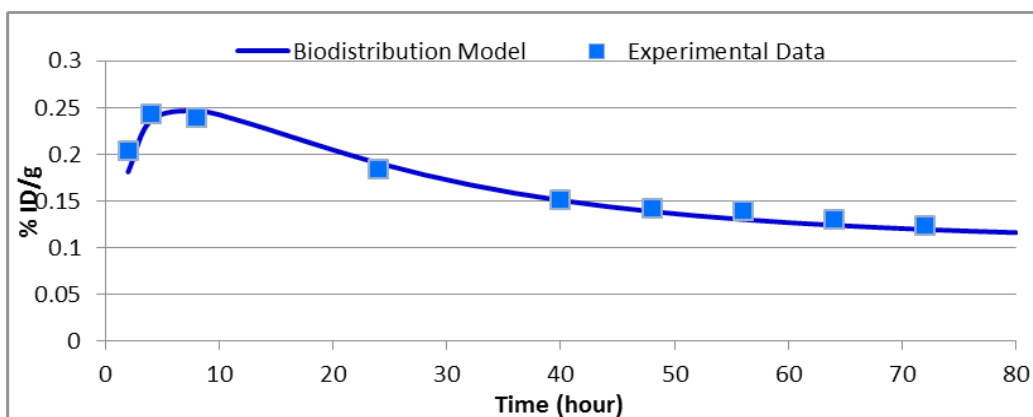


Figure 1. c. Comparison modeling data and biodistribution data for Brain.

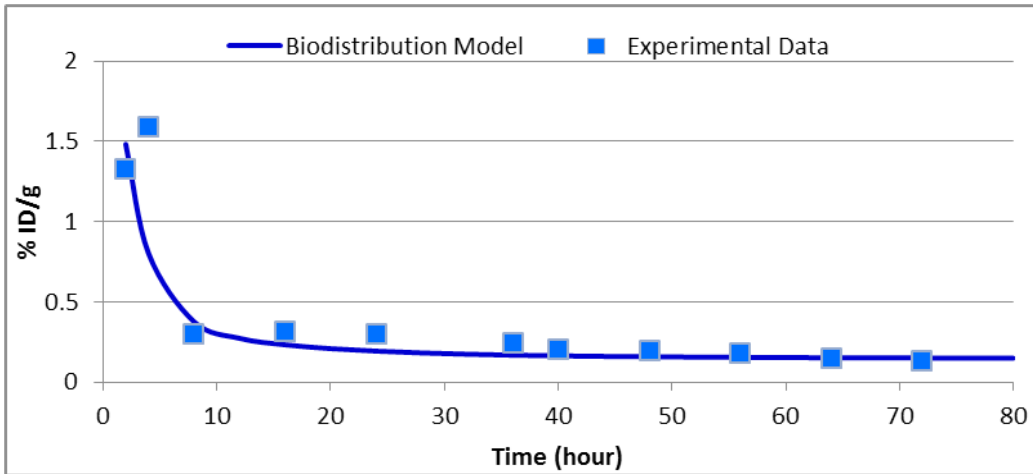


Figure 1. d. Comparison modeling data and biodistribution data for Heart.

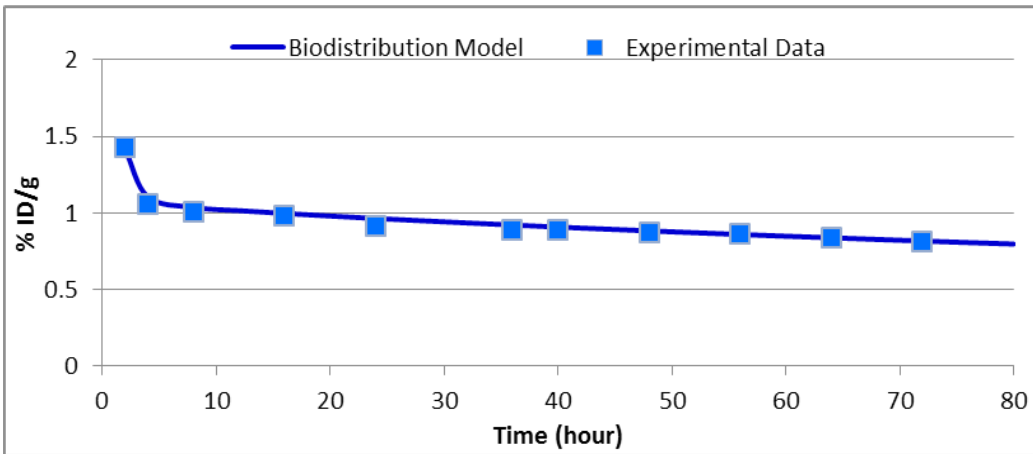


Figure 1. e. Comparison modeling data and biodistribution data for Intestine.

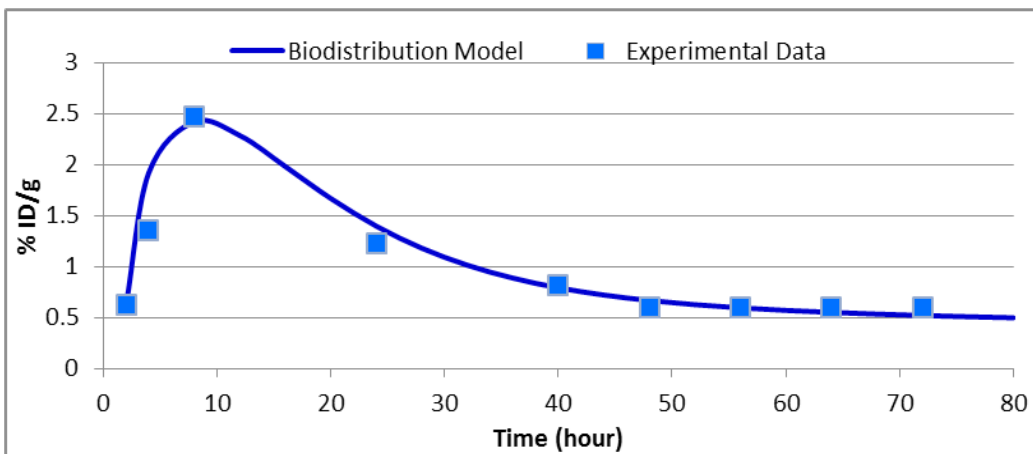


Figure 1. f. Comparison modeling data and biodistribution data for Kidney.

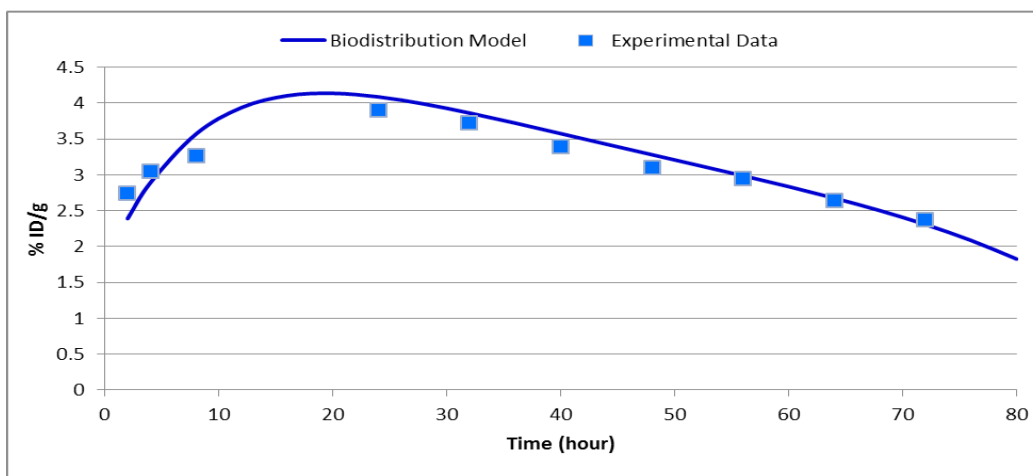


Figure 1. g. Comparison modeling data and biodistribution data for Liver.

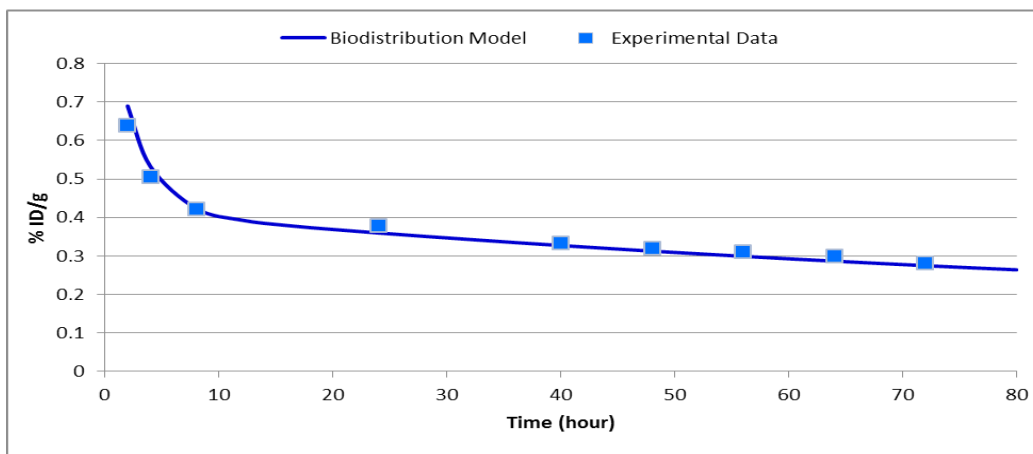


Figure 1. h. Comparison modeling data and biodistribution data for Lung.

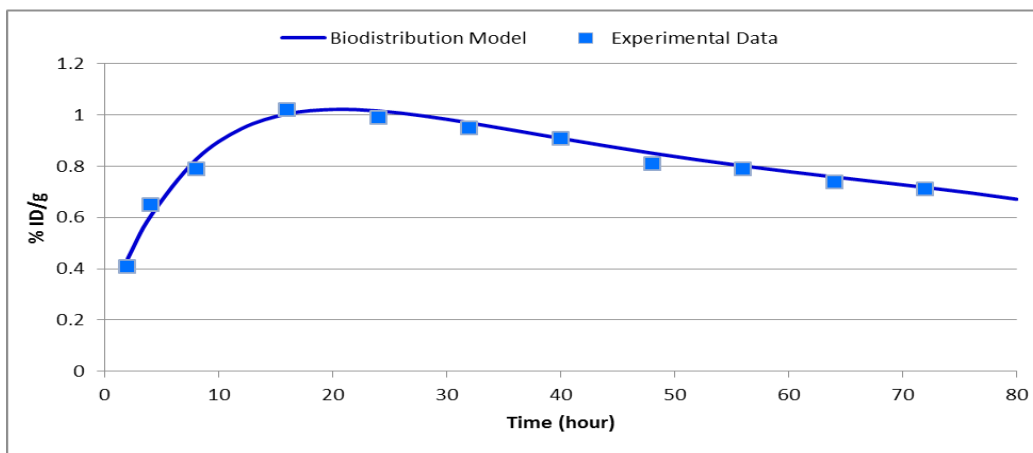


Figure 1. i. Comparison modeling data and biodistribution data for Spleen.

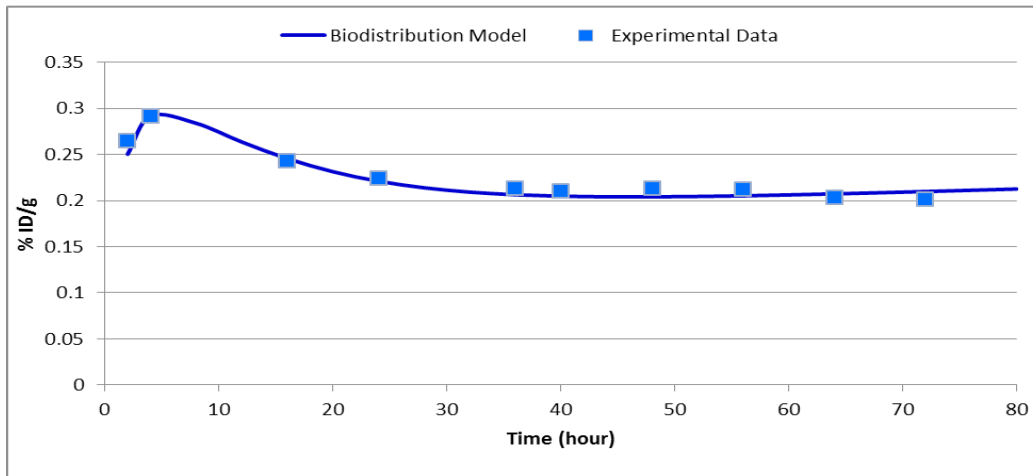


Figure 1. j. Comparison modeling data and biodistribution data for Stomach.

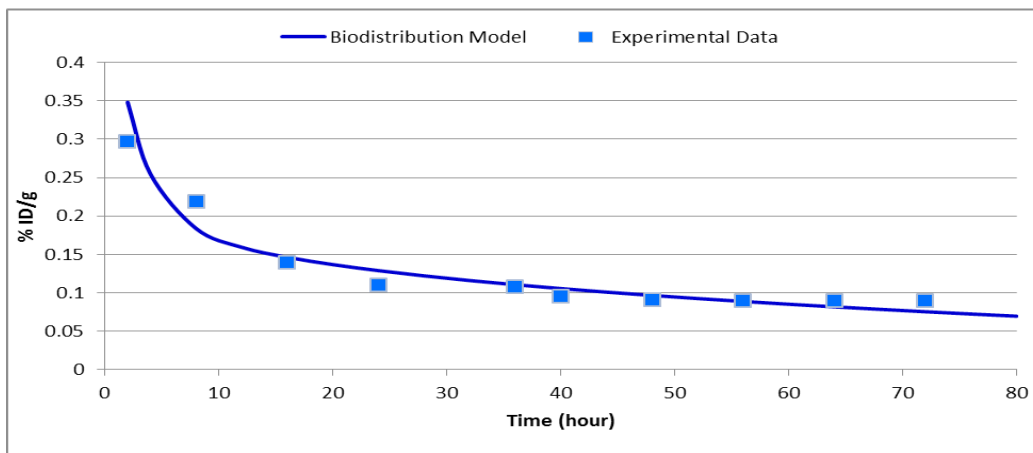


Figure 1. k. Comparison modeling data and biodistribution data for Xhyphoid.

^{166}Ho was used for head and neck cancer pain relief in patients with bone metastases. It was administered proportional to body weight (37 MBq/kg) in 80 patients, 40 of them in combination with external beam radiation therapy. Complete pain relief was observed in 40% of patients, a more satisfactory figure compared with ^{166}Ho [4,5].

Although considered as a negative effect in DOTA, the remarkable concentration of Avastin in the liver makes it a good candidate for treatment of liver cancer. The ID/g concentration of Avastin in the liver is 3.4 times higher than that in bone. One advantage of ^{166}Ho -DOTA is its fast blood clearance (Figure 1. a) in this condition drug were removed from the body very fast because of its fast metabolism.

4. Discussion

Beta emitter radioisotope of a rare earth metal, Holmium, ^{166}Ho , can destroy cancer cells due to its radiation, if deposited inside the tumor. Using nuclear imaging techniques, it was shown that the labeled compound ^{166}Ho -DOTA-Bevacizumab concentrates in tumor tissue and is a proper candidate for targeted radioimmunotherapy. Concentration of ^{166}Ho -DOTA-Bevacizumab in important organs of tumor bearing mice was measured at time intervals of up to 96 h. It was concluded that its concentrated depicts various behaviors as a function of time in different organs. As shown in Figures 1. (a to k) the distribution model has a good coincident with experimental data and it is a good sign for a time modeling for the other experiments to save time and money.

In the blood in experimental data, the concentration of radiopharmaceutical decreases up to 10 h after injection and after that approximately plateau is observed as shown in biodistribution model. In the Bone, the variation is monotonically decreasing and the rate of decrement becomes slower at longer times after injection. In the Brain and Stomach the concentration of radiopharmaceutical increases up to 4 h after injection and after that slow decrement is observed. In the Heart, as the same as the Blood graph at first the sharp decrement up to 10 h after injection and then the plateau is observed. In intestine peak of concentration in 2 h after injection is observed and then decrease slowly at longer time and this is a good concentration sign for uptake of colorectal cells. The same trend observed in the spleen and liver as decrease up to 16 h after injection and then decrease with a constant gradient approximately. In the long as the same as the intestine peak of concentration is 2 h post injection and after that slowly decreases was observed. Concentration in tumor is desirably constant until 72 h after injection and decreases to 78% of the initial value after 96 h. In the spleen, after a rapid increase, a maximum is observed at $t = 16$ h, after which the concentration curve tends to decrease to reach a level a few times lower than the initial one. It is concluded that ^{166}Ho -DOTA-Bevacizumab might be considered in the future as a radiopharmaceutical for targeted radiotherapy of cancerous tissues especially in colorectal cancer. For this purpose, more preclinical stages, such as rabbit experiment and human toxicity tests must be performed. And it may be getting a better result, adjusting with external beam therapy. In comparison with Samarium-153, the same radionuclide in radiotargeted therapy, the Holmium-166 has better beta energy in therapy, but its gamma ray for following treatment process is a little less than Samarium-153 gamma ray. Finally the comparison of biodistribution data in experiments and time modeling has a good joint together and this is a good sign for next research of this field to save a time and expense to achieve a soon results and data for other radiopharmacueticals.

Acknowledgment

The author would like to acknowledge to Mrs Ayoobiyan to a grammatical edition of the manuscript.

References

- 1- Available: <http://www.gene.com/gene/products/information/pdf/avastinprescribing>
- 2- A. Baumann, "Early development of therapeutic biologics-pharmacokinetics," *Curr Drug Metab*, vol. 7, pp. 15-21, Jan 2006.
- 3- B. S. Kuszyk, F. M. Corl, F. N. Franano, D. A. Bluemke, L. V. Hofmann, B. J. Fortman, et al., "Tumor transport physiology: implications for imaging and imaging-guided therapy," *AJR Am J Roentgenol*, vol. 177, pp. 747-53, Oct 2001.
- 4- A. Khorrami Moghaddam, A. Jalilian, K. Yavari, B. Bolouri, A. Bahrami-Samani, and M. Ghannadi-Maragheh, "Production and quality control of [^{166}Ho]-DOTA-bevacizumab for therapeutic applications," *Journal of Radioanalytical and Nuclear Chemistry*, vol. 292, pp. 1065-1073, 2012/06/01.
- 5- A. Khorami-Moghadam, B. Bolouri, A. R. Jalilian, N. M. Bahrami-Samani, S. M. Mazidi, and B. Alirezapour, "Preclinical evaluation of holmium-166 labeled anti-VEGF-A(Bevacizumab)," *J Labelled Comp Radiopharm*, vol. 56, pp. 365-9, Jun 30 2013.
- 6- M. Coronado, A. Redondo, J. Coya, E. Espinosa, R. M. Couto, P. Zamora, et al., "Clinical role of Sm-153 EDTMP in the treatment of painful bone metastatic disease," *Clinical nuclear medicine*, vol. 31, pp. 605-610, 2006.
- 7- H. Zhu, R. J. Melder, L. T. Baxter, and R. K. Jain, "Physiologically based kinetic model of effector cell biodistribution in mammals: implications for adoptive immunotherapy," *Cancer research*, vol. 56, pp. 3771-3781, 1996.
- 8- IAEA, "Manual for reactor produced radioisotopes," 2003.
- 9- M. Bączyk, P. Milecki, P. Martenka, and J. Sowiński, "Efficacy of samarium 153 and strontium 89 treatment for bone metastases in prostate cancer patients: monotherapy vs. treatment combined with external beam radiotherapy. Preliminary report," *Reports of Practical Oncology & Radiotherapy*, vol. 12, pp. 211-216, 2007.

- 10- T. Lindmo, E. Boven, F. Cuttitta, J. Fedorko, and P. Bunn, "Determination of the immunoreactive function of radiolabeled monoclonal antibodies by linear extrapolation to binding at infinite antigen excess," *Journal of immunological methods*, vol. 72, pp. 77-89, 1984.
- 11- H. Yousefnia, E. Radfar, A. R. Jalilian, A. Bahrami-Samani, S. Shirvani-Arani, A. Arbabi, *et al.*, "Development of ¹⁷⁷Lu-DOTA-anti-CD20 for radioimmunotherapy," *Journal of Radioanalytical and Nuclear Chemistry*, vol. 287, pp. 199-209, 2011.
- 12- I. Demir, F. Z. B. Muftuler, P. Unak, and C. Acar, "In vivo investigation of radiolabeled bevacizumab in healthy rat tissues," *Brazilian Archives of Biology and Technology*, vol. 54, pp. 73-79, 2011.
- 13- S. Zolghadri, A. R. Jalilian, H. Yousefnia, A. Bahrami-Samani, S. Shirvani-Arani, and M. Ghannadi-Maragheh, "Preparation and quality control of ¹⁶⁶Ho-DTPA-antiCD20 for radioimmunotherapy," *Radiochimica Acta International journal for chemical aspects of nuclear science and technology*, vol. 99, pp. 237-242, 2011.
- 14- M. Eder, A. V. Krivoshein, M. Backer, J. M. Backer, U. Haberkorn, and M. Eisenhut, "ScVEGF-PEG-HBED-CC and scVEGF-PEG-NOTA conjugates: comparison of easy-to-label recombinant proteins for [⁶⁸ Ga] PET imaging of VEGF receptors in angiogenic vasculature," *Nuclear medicine and biology*, vol. 37, pp. 405-412, 2010.
- 15- M. F. Lima, P. B. Pujatti, E. B. Araújo, and C. H. Mesquita, "Compartmental analysis to predict biodistribution in radiopharmaceutical design studies," 2009.